

Halfway Between CP and Tucker Model: PARALIND Analysis of Human Electroencephalogram

Zuzana Rošťáková, Roman Rosipal, Nina Evetović

Institute of Measurement Science, Slovak Academy of Sciences, Bratislava, Slovakia
Email: zuzana.rostakova@savba.sk

Abstract. Subject-specific narrowband oscillatory rhythms in human electroencephalogram (EEG) can be detected using tensor decomposition. In our previous studies, we explored the CANDECOMP/PARAFAC (CP) decomposition together with the more flexible Tucker model. However, we found that CP decomposition sometimes required a high number of latent components to represent the data latent structure accurately. On the other hand, the Tucker model appeared too generalized, leading to very sparse solutions. Therefore, in this study, we focus on the PARALIND model, which combines the more straightforward interpretability of CP decomposition with the flexibility of the Tucker model. We demonstrate its performance on EEG recordings from a patient following an ischemic stroke, comparing it to the previous two models.

Keywords: Electroencephalogram, Tensor, CP Decomposition, Tucker Model, PARALIND

1. Introduction

The effectiveness of tensor decomposition methods to successfully reveal the latent structure of EEG signal has been proved in our previous study [1], which focused on the CANDECOMP/PARAFAC (CP) decomposition and Tucker model [2, p. 43 and 59]. However, we discovered that CP decomposition needed a considerably higher number of components to effectively represent the latent structure of the data when the EEG signal was recorded using a limited number of electrodes focused on specific brain regions, such as the central sensorimotor cortex [1]. The Tucker model, on the other hand, produced a very sparse decomposition, indicating it is too flexible for the analyzed data. In this study, we, therefore, focus on an alternative model called PARALIND - the parallel profiles with linear dependencies [3] - combining the flexibility of the Tucker model with the intuitive interpretability of the CP decomposition and discuss its performance when detecting narrowband brain oscillatory rhythms.

2. PARALIND and its relationship with other tensor decomposition models

The PARALIND model [3] with (M, N, O) signatures and $F \geq \max\{M, N, O\}$ common components can be described using two equivalent formulas

$$\underline{X} = \underline{A} \times_1 \underbrace{(AH_A)}_{A^*} \times_2 \underbrace{(BH_B)}_{B^*} \times_3 \underbrace{(CH_C)}_{C^*} + \underline{E} = \sum_{f=1}^F \lambda_{fff} \underbrace{(AH_A)_f}_{\mathbf{a}_f^*} \circ \underbrace{(BH_B)_f}_{\mathbf{b}_f^*} \circ \underbrace{(CH_C)_f}_{\mathbf{c}_f^*} + \underline{E}, \quad (1)$$

$$\underline{X} = \underbrace{(\underline{A} \times_1 H_A \times_2 H_B \times_3 H_C)}_{\underline{G}^*} \times_1 A \times_2 B \times_3 C + \underline{E} = \sum_{m=1}^M \sum_{n=1}^N \sum_{o=1}^O \underbrace{\left(\sum_{f=1}^F \lambda_{fff} \mathbf{h}_{mf}^A \mathbf{h}_{nf}^B \mathbf{h}_{of}^C \right)}_{g_{mno}^*} \mathbf{a}_m \circ \mathbf{b}_n \circ \mathbf{c}_o + \underline{E}, \quad (2)$$

where $\underline{X} \in \mathbb{R}^{I \times J \times K}$ denotes a data tensor and $\underline{E} \in \mathbb{R}^{I \times J \times K}$ represents model error. The component matrices $A = [\mathbf{a}_1, \mathbf{a}_2, \dots, \mathbf{a}_M] \in \mathbb{R}^{I \times M}$, $B = [\mathbf{b}_1, \mathbf{b}_2, \dots, \mathbf{b}_N] \in \mathbb{R}^{J \times N}$, $C = [\mathbf{c}_1, \mathbf{c}_2, \dots, \mathbf{c}_O] \in \mathbb{R}^{K \times O}$ represent the temporal (TS), spatial (SpS) and frequency signatures (FS) of the latent components. The relationships between signatures in different modes are captured by the dependency matrices $H_A \in \mathbb{R}^{M \times F}$, $H_B \in \mathbb{R}^{N \times F}$, $H_C \in \mathbb{R}^{O \times F}$. Unlike in [3], where the dependency

matrices were assumed to be known and fixed, we have chosen to estimate them simultaneously along with the component matrices using the alternating least squares algorithm [2].

The core tensor $\underline{\Lambda} \in \mathbb{R}^{F \times F \times F}$ is super-diagonal with $\lambda_{mno} \neq 0$ only if $m = n = o$. The f^{th} column of the matrix product $AH_A = A^*$ is denoted by $(AH_A)_f = \mathbf{a}_f^*$. Finally, $\underline{X} \times_n Y$ represents the tensor-matrix product in the n^{th} mode and $\mathbf{a} \circ \mathbf{b}$ is an outer product of two vectors [2].

Considering Eq. (1), PARALIND is a CP model with F components and component matrices A^*, B^*, C^* . Due to the superdiagonality of $\underline{\Lambda}$, the f^{th} column of A^* is related only with the the f^{th} columns of B^* and C^* . Additionally, PARALIND can also be interpreted as an (M, N, O) -Tucker model with the core tensor \underline{G}^* following a CP structure, as described in Eq. (2) [3].

3. Data

In this study, we focused on the multichannel EEG signal from 13 recordings of an 84-year-old man with post-stroke right-sided hemiplegia [4]. The EEG signals were recorded at a sampling frequency of 250 Hz, using 10 electrodes positioned over the sensorimotor area¹ and referenced to linked ears. Following [1], we inspected and corrected potential artefacts semi-automatically using the BrainVision Analyser 2 software.

For each recording day, the EEG signal was divided into overlapping two-second time windows. For each time window, we computed the oscillatory part of the amplitude spectrum, and the \log_{10} -transformed values were concatenated into a tensor $\underline{X} \in \mathbb{R}^{I \times J \times K}$, where I, J , and K represent the number of time windows, the number of electrodes, and the number of frequencies, respectively. Before tensor decomposition, the tensor \underline{X} was centered in the first mode.

To be consistent with [1], we applied the nonnegativity constraints for TS and SpS, as well as unimodality constraints for FS in the CP decomposition, Tucker model, and PARALIND. Based on our earlier findings [1], we expected the lateralization of latent components - a different temporal activation of the same brain oscillation in the left and right hemisphere. Therefore, we selected the number of signatures in the various models as follows:

- CP with F components (F signatures in all three modes),
- Tucker model with either $(F, 2, F)$ or $(F, 2, \frac{F}{2})$ signatures (denoted as T1 and T2),
- PARALIND with F common components and $(F, 2, F)$ or $(F, 2, \frac{F}{2})$ signatures (PL1, PL2).

Here, F is an even number ranging from four to 20, which leads to nine CP, PL1, PL2, T1, and T2 models for each training day.

4. Results

The suitability of the PARALIND application was validated by two main observations: first, the presence of duplicate components in the CP decomposition, which indicated the same oscillation occurring with different temporal activities in both hemispheres; second, the trilinear and sparse structure of the core tensors \underline{G} in both Tucker models, where the percentage of nonzero elements ranged from 5% to 25%. The trilinear structure of $\underline{G} \in \mathbb{R}^{F \times 2 \times \frac{F}{2}}$ in T2 was confirmed by the core consistency diagnostics (CCD) [2, p. 78], which was close to or equal to 100% for all days assessed. The ratio of the T1 core tensors with CCD values exceeding the 90% threshold (indicating pure trilinearity) varied from 0.44 on Day 10 to 1 on Days 2 and 9, with a mode of 0.89 observed over five days.

In the next step, we compared the mean squared error (MSE) across models with the same number of common components F . As depicted in Fig. 1, the CP, T1, and PL1 models achieved

¹Electrode placement followed the 10-20 system, with electrodes positioned at FC3, C1, C3, C5, CP3, and FC4, C2, C4, C6, CP4.

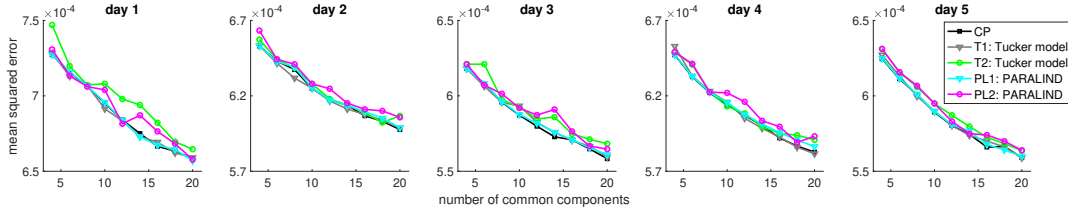


Fig. 1: The mean squared error of CP and two versions of both the Tucker model and PARALIND with the number of common components $F \in \{4, 6, \dots, 20\}$ when applied to the first five recording days.

similar MSE values. The slightly higher MSE observed in T2 and PL2 (Fig. 1, green and magenta) was expected, as these models used half the number of FS compared to the corresponding CP, PL1, and T1. Another reason could be that the T2 and PL2 structure is more restricted to laterality. Nonetheless, from a quantitative point of view, we can conclude that both versions of PARALIND modeled the data latent structure comparably to the CP and Tucker model.

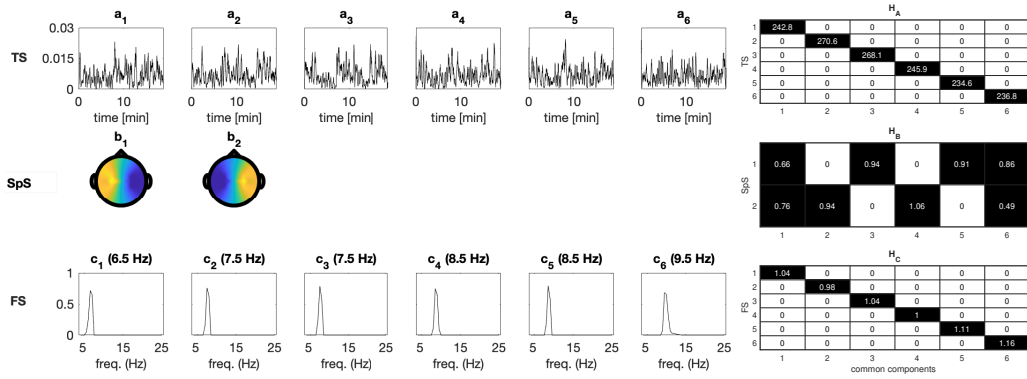


Fig. 2: Day 12 - PARALIND model PL1 with (6,2,6) signatures and six common components. The component signatures are depicted on the left, and the dependency matrices H_A, H_B, H_C are on the right.

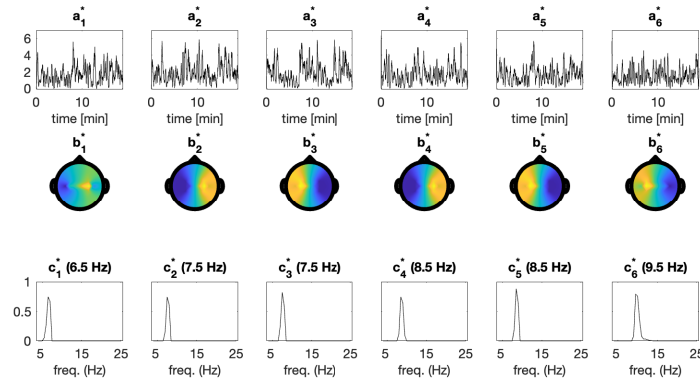


Fig. 3: Day 12 - Common component signatures from the PARALIND model PL1 depicted in Fig. 2.

The interpretability of the PARALIND decomposition is also essential. Let us examine the outcome of the PL1 model with (6, 2, 6) signatures and $F = 6$, applied to data from Day 12 (Fig. 2). Two SpS represent oscillatory activity in the left and right hemisphere (Fig. 2, left, middle row). Observing six FS, we notice some duplicates, such as two instances of 8.5 Hz and 7.5 Hz, a phenomenon also found in CP decomposition. By examining the nonzero elements in the first columns of dependency matrices (Fig. 2, right), we found that the first latent component oscillates at 6.5 Hz (FS c_1), with its time score corresponding to a_1 and spatial representation

given by the linear combination of two SpS: $b_1^* = 0.66b_1 + 0.76b_2$. Additionally, an analysis of the second and third, or fourth and fifth columns of the dependency matrices shows that these latent components represent a lateralized version of the 7.5 Hz and 8.5 Hz rhythms. Moreover, PL1 can be easily represented in a CP-like structure (Fig. 3).

The dependency matrices of the PL2 model with (6, 2, 3) signatures and $F = 6$ revealed a sparse structure that effectively highlights the lateralization of three oscillatory rhythms on 7, 8.5, and 9.5 Hz (Fig. 4). For example, the first two latent components represent 9.5 Hz rhythm (FS c_1), observed both in the left (SpS b_1 , TS a_2) and in the right hemisphere (SpS b_2 , TS a_4).

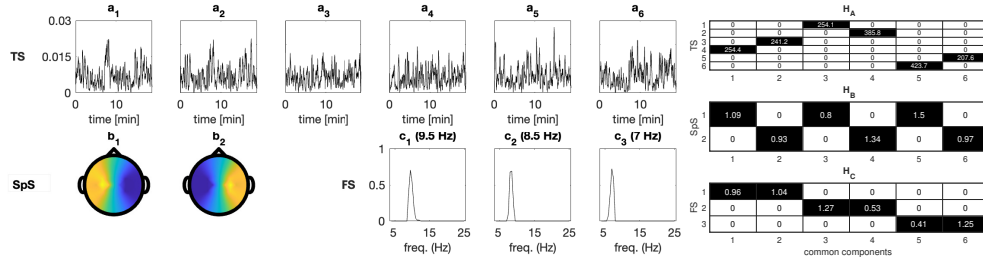


Fig. 4: Day 12 - PARALIND model PL2 with (6,2,3) signatures and six common components. The component signatures are depicted on the left, and the dependency matrices H_A, H_B, H_C are on the right.

5. Conclusion

This study explored the potential use of the PARALIND model for detecting narrowband brain oscillatory rhythms in EEG signal. The validity of PARALIND was supported by duplicate components estimated through CP decomposition, the trilinear structure of the core tensor in Tucker models, and comparable MSE across all models when applied to the same data. An important advantage of PARALIND is its straightforward representation in a CP-like structure, where each latent component is defined by its TS, SpS, and FS. Additionally, its dependency matrices provide a more intuitive interpretation compared to the core tensor in the Tucker model. A limitation of PARALIND are numerical instabilities when estimating dependency matrices and challenging selection of the appropriate number of signatures, highlighting the need for future research in this area.

Acknowledgements

Funded by the EU NextGenerationEU through the Recovery and Resilience Plan for Slovakia under the project No. 09I03-03-V04-00205 (Z.R.) and project No. 09I03-03-V04-00443 (R.R.). N.E. received funding from the HORIZON-MSCA-2022-DN, 101118964-DONUT project.

References

- [1] Rošťáková, Z., Rosipal, R., Seifpour, S., Trejo, L. J. (2020). A comparison of non-negative Tucker decomposition and parallel factor analysis for identification and measurement of human EEG rhythms. *Measurement Science Review* 20(3), 126 – 138.
- [2] Cichocki, A., Zdunek, R., Phan, A. H., Amari, S. (2009). *Nonnegative matrix and tensor factorizations: applications to exploratory multi-way data analysis and blind source separation*. United Kingdom: John Wiley & Sons.
- [3] Bro, R., Harshman, R. A., Sidiropoulos, N. D., Lundy, M. E. (2009). Modeling multi-way data with linearly dependent loadings. *Journal of Chemometrics: A Journal of the Chemometrics Society* 23(7-8), 324–340.
- [4] Polyanskaya, A., Rosipal, R., Sobolová, G., Rošťáková, Z., Porubcová, N. (2024). A small step towards the detection of mental fatigue induced by BCI-HMD training. In: *Proceedings of the 9th Graz Brain-Computer Interface Conference 2024*. pp. 109–114.